AGU PUBLICATIONS

Geophysical Research Letters

RESEARCH LETTER

10.1002/2015GL063755

Key Points:

- Plasmaspheric hiss originates in the plasmaspheric drainage plumes
- Hiss is absorbed in the equatorial region of the plasmasphere
- Hiss source is limited to the equatorial region of plumes

Correspondence to:
H. Laakso,
harri.laakso@esa.int

Citation:
Laakso, H., O. Santolik, R. Horne, I. Kolmasová, P. Escoubet, A. Masson, and M. Taylor (2015), Identifying the source region of plasmaspheric hiss, *Geophys. Res. Lett.*, *42*, 3141–3149, doi:10.1002/2015GL063755.

Received 9 MAR 2015
Accepted 15 APR 2015
Accepted article online 21 APR 2015
Published online 13 MAY 2015

Identifying the source region of plasmaspheric hiss

Harri Laakso[1], Ondrej Santolik[2], Richard Horne[3], Ivana Kolmasová[4], Philippe Escoubet[1], Arnaud Masson[5], and Matthew Taylor[1]

[1]ESTEC, European Space Agency, Noordwijk, Netherlands, [2]Institute of Atmospheric Physics CAS, Prague, Czech Republic, [3]British Antarctic Survey, Natural Environment Research Council, Cambridge, UK, [4]Faculty of Mathematics and Physics, Charles University Prague, Czech Republic, [5]ESAC, European Space Agency, Madrid, Spain

Abstract The presence of the plasmaspheric hiss emission around the Earth has been known for more than 50 years, but its origin has remained unknown in terms of source location and mechanism. The hiss, made of whistler mode waves, exists for most of the time in the plasmasphere and is believed to control the radiation belt surrounding the Earth which makes its understanding very important. This paper presents direct observational evidence that the plasmaspheric hiss originates in the equatorial region of the plasmaspheric drainage plumes. It shows that the emissions propagate along the magnetic field lines and away from the equator in the plumes but toward the equator at lower L shells inside the plasmasphere. The observations also suggest that the hiss waves inside the plasmasphere are absorbed as they cross the equator.

1. Introduction

The plasmasphere, consisting of cold ions and electrons of atmospheric origin, extends up to a distance of about 4 Earth's radii at the equator; the actual distance of the edge of the plasmasphere, called the plasmapause, varies strongly with local time and geomagnetic activity [*Chappell et al.*, 1970]. In addition, the plasmasphere is affected by a variety of erosion processes that transport the cold plasmaspheric particles into the hot and tenuous magnetosphere. This occurs particularly in the dusk sector where the plasmasphere is eroded via plasmaspheric drainage plumes [*Elphic et al.*, 1996]. Although the formation of plumes has still plenty of open issues, it is basically related to the time-varying convection electric fields in the magnetosphere. Due to the Earth's magnetic field, the plasmaspheric cold plasma corotates with the Earth. At a certain distance, near the plasmapause, the magnetospheric electric fields exceed the corotation electric field, and in the dusk sector, they point into the opposite direction. As a result, the plasmaspheric plasma can drift into the magnetosphere which appears as a large-scale plume. In the plume, the charged particles drift away from the plasmasphere toward the dayside magnetopause under the influence of magnetospheric convection [*Walsh et al.*, 2013]. The plumes can be observed in all local time sectors and in all geomagnetic conditions [*Darrouzet et al.*, 2008], although their characteristics (size, density, etc.) can vary significantly. The plumes appear to sustain strong hiss emission for most of the time, similarly to the plasmasphere itself [*Summers et al.*, 2008].

The plasmaspheric hiss was first detected by low- and high-altitude spacecraft in the 60s which resulted in a large number of studies and theories on its characteristics and origin [*Thorne et al.*, 1973]. However, its origin has remained unknown to the present day in terms of source location and mechanism. Several mechanisms have been proposed to be responsible for the hiss generation [*Bortnik et al.*, 2008; *Santolík and Chum*, 2009; *Meredith et al.*, 2013], although many of them have difficulties to explain the observed characteristics and variations of the hiss emission.

The hiss emission is important because it is believed to cause loss of energetic trapped particles, resulting in a slot region within the radiation belts around the Earth [*Lyons and Thorne*, 1973; *Meredith et al.*, 2007]. Hiss is regularly observed in the inner magnetosphere, particularly in the plasmasphere. This paper presents direct observational evidence that the hiss emission is generated in the equatorial region of plasmaspheric drainage plumes in the dusk sector, and in the plasmasphere, the hiss waves propagate toward the equator on both hemispheres. Furthermore, the simultaneous observations in the plasmasphere around the magnetic equator suggest that the hiss waves are absorbed at the equator.

2. Observations

The Cluster mission, consisting of four identical polar-orbiting satellites [*Escoubet et al.*, 2001], offers an excellent opportunity to look at the details of the hiss emission. The satellite trajectories are 56 h long, and

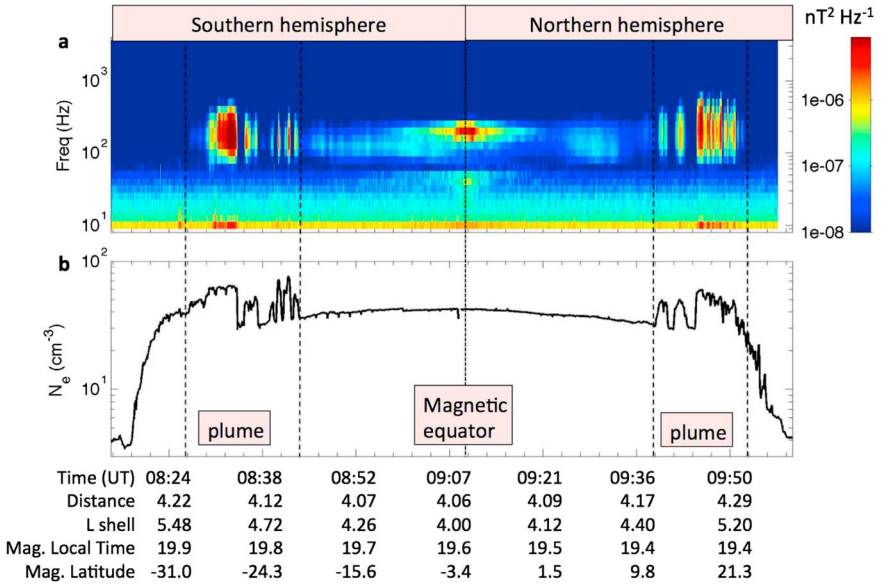

Figure 1. Plasma waves around the magnetic equator, detected by Cluster 1 on 8 May 2001 while moving from the southern hemisphere to the northern hemisphere. (a) Total power spectral density of wave magnetic fields, color coded according to the color bar on the right-hand side. (b) Total electron density. The density shows a large-scale density enhancement in both hemispheres, which are all related to the presence of a plasmaspheric plume.

at two points along the orbit, the constellation forms a perfect tetrahedron configuration. At other points along the trajectory, the constellation is a more or less deformed tetrahedron, and near the perigee, the four satellites follow each other in a string-of-pearls configuration. In May 2001, the tetrahedron had a 600 km separation between the satellites, and then at perigee, the four satellites followed each other within about 10 min. In the perigee region, the spacecraft cross the inner magnetosphere and often encounters the plasmaspheric region.

Figure 1 shows the electron density (Figure 1b) and wave magnetic field observations (Figure 1a) from Cluster 1 on 8 May 2001 when the spacecraft moved from the southern into the northern hemispheres in the dusk sector (19:00–20:00 magnetic local time (MLT)). The electron density has been derived from the spacecraft potential measurements. This conversion has been done with help of the absolute electron density measurements from the Waves of High frequency and Sounder for Probing of Electron density by Relaxation (WHISPER) experiment during this interval. WHISPER density data have much lower cadence than EFW spacecraft potential data, but there are enough simultaneous data points of spacecraft potential and density in the range of 1–100 cm^{-3}, which are used to create a function to convert the spacecraft potential into the electron density. On the horizontal axis below time, spacecraft positional information is given: distance is the geometric distance from the center of the Earth in Earth's radius, L shell, magnetic latitude, and magnetic local time based on the tilted dipole field model.

This pass shows typical signatures of the plasmaspheric drainage plume which have been studied in great detail with Cluster and IMAGE satellites in the past decade [*Darrouzet et al.*, 2006, 2008]. One can recognize the main plume and some small-scale features on the earthward side of the plume. In both hemispheres, two vertical dashed lines are drawn to indicate the densest plume region. The outer edge of the plume has quite a smooth and steep density gradient that is also a typical feature of the plume. One can also see that the strongest hiss emission is limited in the densest plume region and that the hiss power spectral density decreases with electron density. Overall, this is a typical example of the perigee pass by Cluster in the dusk sector where both a plume and hiss emission are detected.

Note that there is no plasmapause crossing in this pass. After passing the plume at 08:45 UT in the southern hemisphere, the density does not change much before the plume is crossed again in the northern hemisphere at about 09:40 UT. Between the two plume crossings, the spacecraft moves along the nearly same L shell around the equator, spacecraft never goes below L = 4.0. The density remains constant,

approximately 30 cm^{-3}, which is quite high and can be considered a good value for the plasmapause region. However, no proper plasmapause crossing happens because this would mean that the density exceeds 100 cm^{-3}, and in this case, the spacecraft should have gone to lower L shells to encounter the proper plasmasphere.

The electromagnetic emission in Figure 1a exhibits two distinct features: the strong wave emission in the plume and at the magnetic equator. Although these two emissions appear partially in the same frequency range, their polarization characteristics are different. The equatorial emission, called equatorial noise [*Němec et al*., 2006], is made of linearly polarized magnetosonic waves, whereas the plume emission, called the plasmaspheric hiss, is made of right-hand circularly polarized whistler mode waves. The crossing of the magnetic equator is well marked by an enhanced magnetosonic emission below 300 Hz at the magnetic equator. The polarization measurements indicate that these waves propagate mainly across the magnetic field which suggests that they are magnetosonic waves, although the latitude range of emission is somewhat larger than that usually associated with magnetosonic waves. The larger-latitude range could be due to a large-density gradient that could help refract the waves to higher latitudes. In this study we use the central point of the emission to mark the magnetic equator.

2.1. Source of Hiss Emission

In order to understand the characteristics of the wave emissions, simultaneous electric and magnetic field measurements are collected by the Spatio-Temporal Analysis of Field Fluctuations experiment on the Cluster spacecraft [*Cornilleau-Wehrlin et al*., 1997]. Based on two electric and three magnetic components, the spectrum analyzer calculates spectral matrix (5×5) in 27 frequency channels between 8 Hz and 4 kHz every 4 s. Note that the third electric field component parallel to the spin axis is not measured. These data are further analyzed on the ground using the singular value decomposition method [*Santolik et al*., 2003]. Figure 2 presents the results of this analysis for the interval of Figure 1.

Figure 2f shows the total power spectral density of the wave magnetic fields which is the same as Figure 1a except that in Figure 2f, the measurements have been filtered out when the wave power is weak (total magnetic power spectral density is less than 10^{-8} nT^2/Hz) or when the wave is not well circularly right-hand polarized (ellipticity is less than +0.7); such data points appear as white area in all panels of Figure 2. The reason for the first filter is that for weak waves, the wave characteristics have too much uncertainties and values become random. The reason for the second filter is that magnetosonic waves occur in the same frequency band with plasmaspheric hiss, and since they are well known to propagate across the magnetic field with linear polarization, these waves are removed to better identify plasmaspheric hiss. Figure 2g shows the total power spectral density of 2-D wave electric fields which displays the same structures as wave magnetic fields, as the whistler mode waves are electromagnetic. The hiss emission in both plume crossings, separated by approximately 1.5 h, appears to have similar power spectral densities. It is also important to note that the hiss power appears in the same frequency range in the plume and in the plasmapause region.

Figure 2e shows the normalized Poynting flux component (normalized against its standard deviation) parallel to the magnetic field. Positive values (shown in red color) indicate that the Poynting flux is parallel to the magnetic field while negative values (shown in blue color) are for antiparallel direction. This figure reveals very important feature of the hiss emission in the plume: the waves propagate poleward over both the southern and northern hemispheres, as indicated by the Poynting flux before ~08:44 UT and after ~09:39 UT. This means that the whistler mode waves propagate away from the equator toward the polar region over both hemispheres. The plumes are crossed approximately at 30° of magnetic latitude, and thus, the source of these waves is equatorward of this position. Furthermore, one can recognize an opposite behavior at lower L shells near the equator (between 08:44 and 09:39 UT), where the spacecraft are near the plasmapause region and where the whistler mode waves propagate toward the equator over both hemispheres.

Figures 2a and 2b show the azimuthal (ϕ_k) and polar (θ_k) angles, respectively, of the direction of the wave vector with respect to the local magnetic field. Figure 2b shows that in the plumes, the wave vector is almost parallel to the magnetic field vector while at lower L shells, the wave vector is more inclined, suggesting that the waves observed in the plumes are closer to the source region [*Santolik et al*., 2010, 2014] while the waves at lower L shells have been refracted. Note that the wave vector angles in Figures

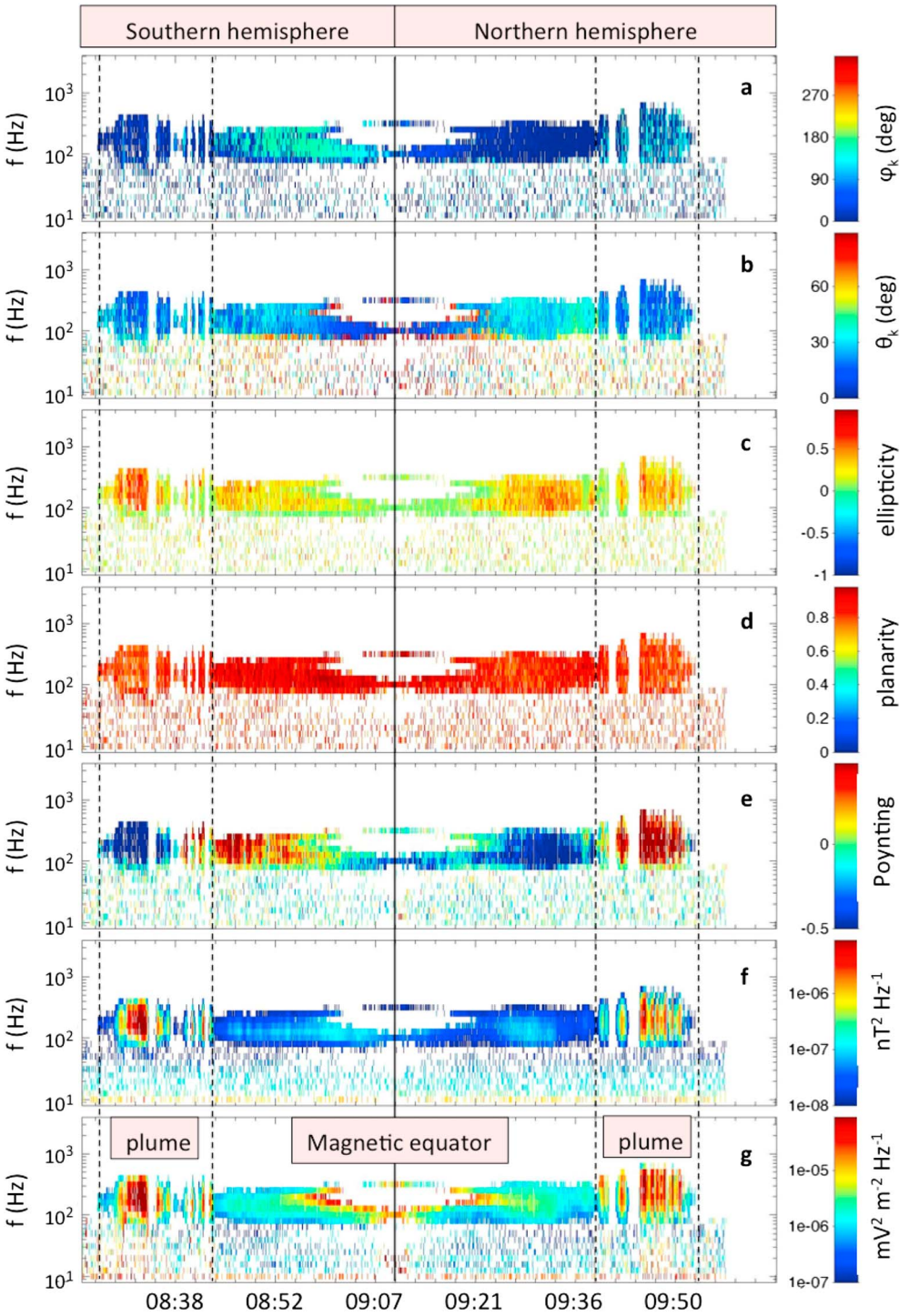

Figure 2. Characteristics of plasma waves measured by Cluster 1 on 8 May 2001, 08:00–10:00 UT. (a and b) Azimuthal and polar angle of the direction of the wave vector with respect to the normal direction to the magnetic field polarization plane. (c) Ellipticity of polarization. (d) Degree of planarity of the polarization plane. (e) Parallel component of the Poynting vector normalized by its standard deviation. (f) Total power spectral density of the 3-D wave magnetic fields. (g) Total power spectral density of the 2-D wave electric fields. In these panels, the data points are filtered out if the magnetic wave power spectral density is low (less than 10–8 nT^2/Hz) or the waves are not right-hand polarized (ellipticity is less than +0.7).

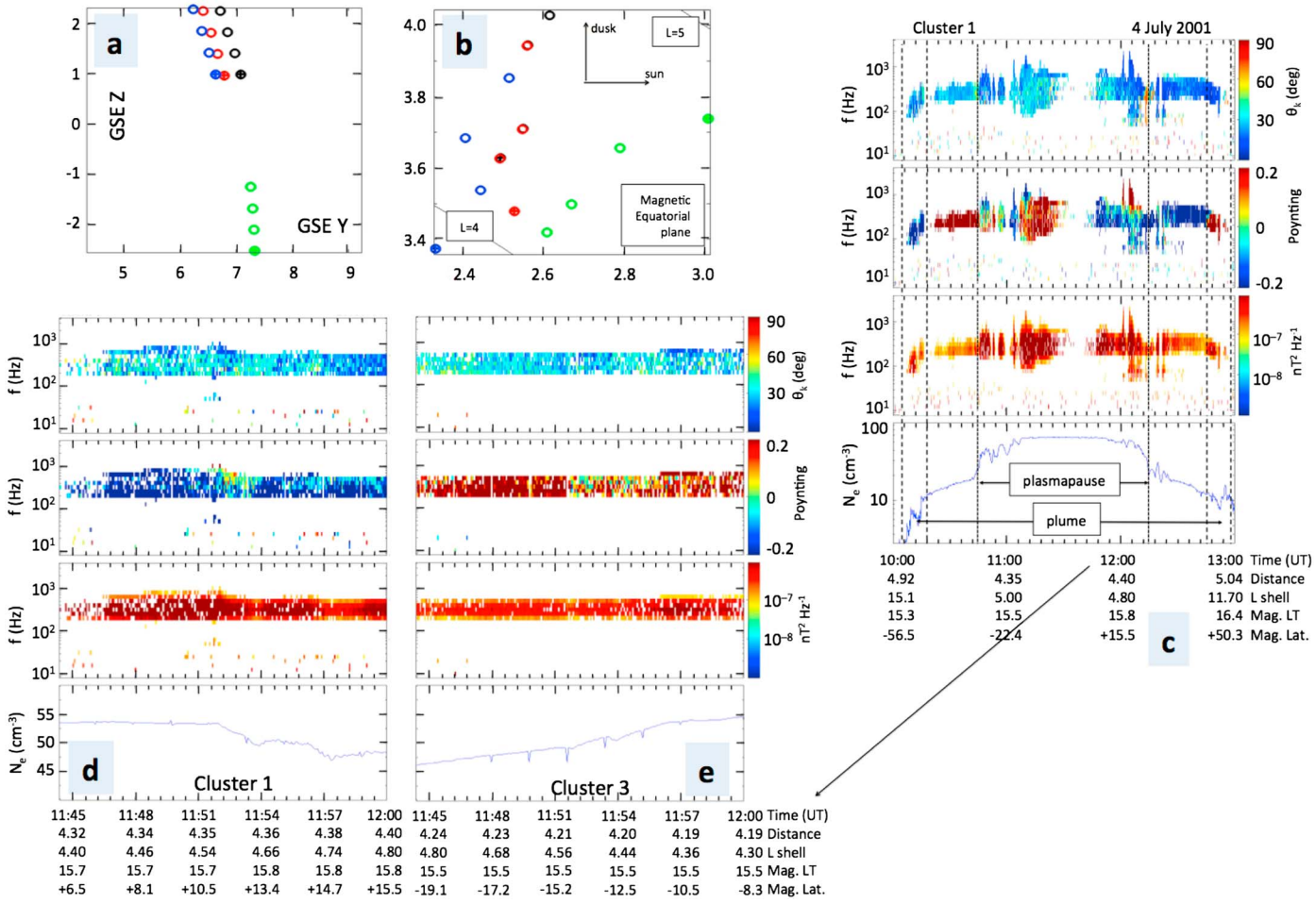

Figure 3. Characteristics of hiss emission in the plasmasphere, as detected by the Cluster spacecraft on 4 July 2001. (a) The spacecraft positions in the GSE *z-y* plane at 11:45–12:00 UT at 5 min intervals (values are in Earth's radius). The solid circles show the first data points; color coding: Cluster 1–4 are shown by black, red, green, and blue, respectively. (b) The foot points of the Cluster spacecraft in the magnetic equator during 11:45–12:00 at 5 min intervals. (c) Hiss observations by Cluster 1 during the perigee pass. The four plots from bottom to top are electron density, total magnetic power spectral density, Poynting flux along magnetic field, and polar angle of k-vector. (d and e) Same as in Figure 3c for Cluster 1 and 3, respectively, at 11:45–12:00 UT.

2a and 2b have been derived from measurements of the magnetic field fluctuations and have therefore an ambiguity of 180°. The sign of the parallel component of the Poynting vector in Figure 2e resolves this ambiguity; for its negative values, the wave vector direction should be interpreted as antiparallel with respect to the results in Figures 2a and 2b, assuming the validity of the plane wave approximation.

Figures 2c displays the ellipticity of polarization indicating that the hiss waves are nearly circularly right-hand polarized. Figure 2d displays the degree of planarity of polarization. It can vary between 0 and 1, where 1 means that the normal of the magnetic field polarization plane of all waves have the same direction and 0 means that the normal direction varies randomly. One can see that most of the hiss waves have a high planarity everywhere, suggesting that waves propagate into the same direction in all regions. This may be somewhat surprising as one may expect that the wave direction should vary quite significantly due to many reflections of whistler mode waves between two hemispheres.

2.2. Absorption of Hiss Emission

The observations on 8 May 2001 were collected during moderate geomagnetic conditions. The *AE* index that represents the global geomagnetic activity varies between 300 and 400 nT during the observations. An hour earlier, there is a weak substorm intensification where *AE* increases briefly from ~200 nT to ~600 nT. The statistical plasmapause models [*Carpenter and Anderson*, 1992; *Moldwin et al.*, 2002, 2004] suggest that the

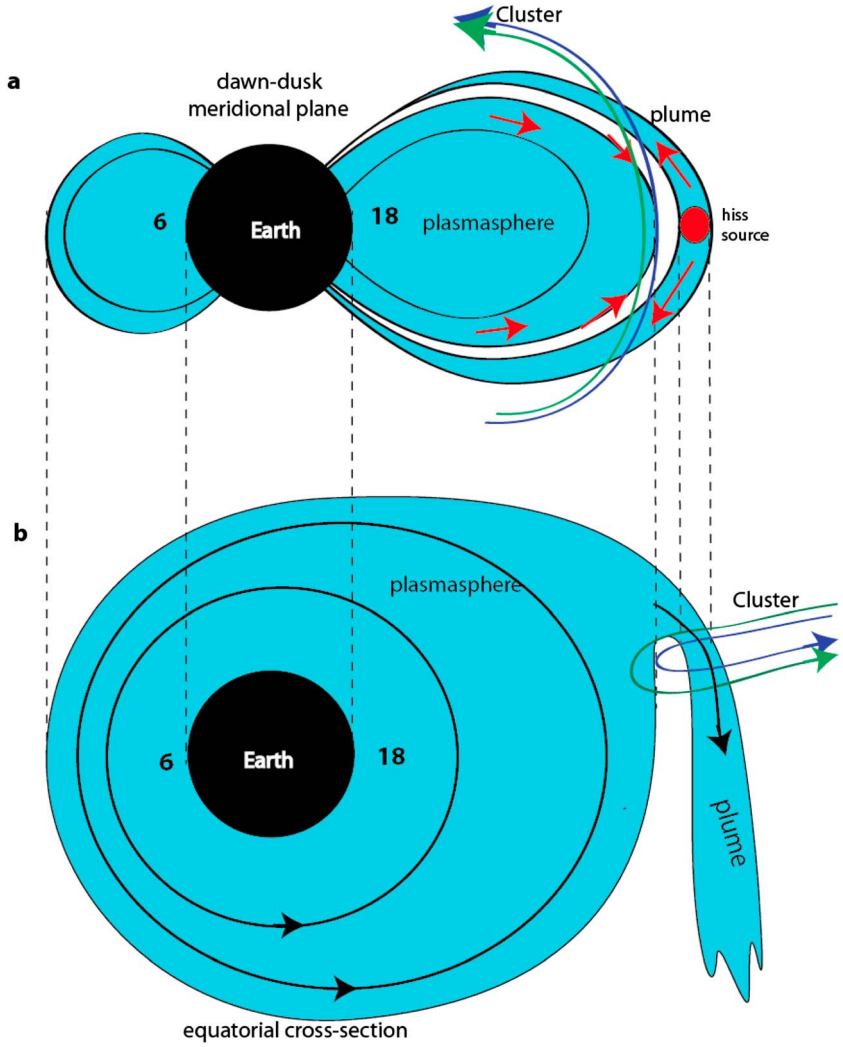

Figure 4. Source of plasmaspheric hiss emission. In the dusk sector, the plasmaspheric drainage plume exists regularly, and it sustains the generation of the hiss emission. (a) Schematic drawing of the inner magnetosphere in the dawn (06:00 LT)-dusk (18:00 LT) meridional plane. The polar-orbiting Cluster spacecraft cross the same plume in both hemispheres at about 30° of magnetic latitude, and the hiss is always observed to propagate away from the equator, as indicated by red arrows. Between two plume encounters, the spacecraft are at lower latitudes and closer to the Earth where the hiss is observed to propagate toward the equator, indicated by red arrows. The blue line represents the spacecraft orbits for Figures 1 and 2, while the green one is for the event of Figure 3. (b) The equatorial cross section of the inner magnetosphere. The blue and green lines show the spacecraft position mapped to the equator along the magnetic field lines. The solid black lines show the convection lines: in the plasmasphere, the plasma corotates with the Earth, and in the plume, plasma convects away from the Earth toward the magnetopause under the influence of the magnetospheric convection electric field.

plasmapause is at L = 4.5 at this local time sector during *Kp* = 2+. However, no plasmapause crossing occurs in this pass. It is quite likely that a substorm before the observation interval was associated with an enhanced magnetospheric convection that caused the erosion of the plasmasphere placing the plasmapause position closer to the Earth. Concerning plasmapause model predictions, one must note that they are statistical and are related only to *Kp* or another geomagnetic index. Thus, it is not a surprise that their predictions do not fit well to the real data because the real plasmapause location depends on several other parameters, most importantly on the magnetospheric convection electric field.

Therefore, we have selected another perigee pass, on 4 July 2001, during which the geomagnetic activity was again stable but now somewhat lower in magnitude (*AE*~100–200 nT). Indeed, this time, the plasmasphere has expanded outward, and the spacecraft are immersed in the plasmaspheric plasma in the perigee region. There is a small difference in spacecraft configuration during this time. Namely, during 10 May to 3

June 2001, the Cluster tetrahedron configuration was changed from 600 km to 2000 km separation. As a consequence, the spacecraft separations at the perigee are such that three spacecraft follow each other rather closely while one, Cluster 3, travels about 45 min behind the other three spacecraft. This creates an interesting configuration around the equator for an interval of 10–15 min, where three spacecraft over the northern hemisphere are magnetically conjugated with Cluster 3 over the southern hemisphere.

Figure 3 presents the observations for the perigee pass of 4 July 2001. Figure 3a shows the spacecraft positions in the GSE *z-y* plane at 11:45–12:00 UT at 5 min intervals (values are in Earth's radius). The solid circles show the first data points; color coding is such that Cluster 1–4 are shown by black, red, green, and blue, respectively. The magnetic equator is crossed by Cluster 3 at about 12:10 UT while the other three spacecraft had crossed it around 11:30 UT (the crossing times are identified by the presence of equatorial noise), so during this interval, Cluster 3 is south of the magnetic equator while the other three are north of the magnetic equator. Figure 3b shows the foot points of the Cluster spacecraft in the magnetic equator during 11:45–12:00 at 5 min intervals, indicating that all spacecraft are mapped into the same region.

Figure 3c presents an overview of hiss observations from Cluster 1 for the overall perigee pass where the plots from bottom to top are electron density, total magnetic power spectral density, Poynting flux along magnetic field, and polar angle of k-vector. Two plasmapause crossings are observed approximately at 10:45 UT and 12:15 UT. There are also weak signatures of plumes, indicated by two vertical dashed lines in both hemispheres. The plumes are observed as localized density enhancements which however are weak because in the late afternoon sector (~16:00 MLT), the plumes are located at large L shells (~10), where the flux tube volumes are very large, reducing the local electron density. The normalized Poynting flux observations in Figure 3c (second panel from top) show the same behavior as Figure 2e: the whistler mode waves propagate away from the equator in the plume, whereas at lower L in the plasmasphere, the waves propagate primarily toward the equator in both hemispheres.

Figures 3d and 3e show the details of hiss observations for Cluster 1 and 3, respectively, at 11:45–12:00 UT, when the two spacecraft are magnetically conjugated on two sides of the magnetic equator (between L = 4–5), as indicated in Figures 3a and 3b. During this interval, the two spacecraft are at magnetic latitudes of about 10–20° in opposite hemispheres. The panels are the same as in Figure 3c. The normalized Poynting flux shows that the whistler mode waves of hiss emission propagate equatorward in both hemispheres at the same time. This is not expected from ray tracing models because the whistler mode waves should bounce between two hemispheres in the plasmasphere; thus, the waves should cross the equator, and the same propagation direction should be seen in both sides of the equator. Now, however, the data suggest that the waves do not cross the equator or at least they are strongly absorbed. Otherwise, the other panels in Figures 3d and 3e show that the both spacecraft observe similar wave characteristics. It is important to note that the polar angles are surprisingly large (30–50°), indicating that near the equator, the waves propagate at oblique angles with respect to the magnetic field. At the equator, the waves are dominated by the equatorial noise, and the whistler mode waves are not seen.

3. Discussion

Overall, the key observation in Figures 1–3 is that the whistler mode waves of the hiss emission are observed to propagate poleward in the plasmaspheric drainage plumes in both hemispheres, whereas in the plasmasphere, the same waves are observed to propagate equatorward, even at 10° of magnetic latitude, and simultaneously in both hemispheres. These observations are summarized in the illustration of Figure 4, where the red arrows present the propagation direction of hiss emission. Figure 4a shows the inner magnetosphere in the dawn (06:00 LT)-dusk (18:00 LT) meridional plane. In the dusk sector, the plasmasphere expands, and a plasmaspheric drainage plume is often formed. The plume consists of flux tubes that connect two hemispheres and that drift sunward (out from the drawing plane). The blue and green lines illustrate Cluster trajectories: the blue line represents the case of Figures 1 and 2 where the spacecraft skims the plasmapause region, whereas the green line represents the observations of Figure 3 where the spacecraft enters the plasmasphere. Figure 4b illustrates the situation in the equatorial plane where blue and green lines represent the Cluster position mapped to the magnetic equator along the magnetic field lines. In the plasmasphere, the cold plasma corotates around the Earth as indicated by black solid lines in Figure 4b, whereas in the plume region, the plasma drifts away from the Earth toward

the magnetopause under the influence of the magnetospheric convection electric field. All perigee passes in spring-summer 2001 (about 20 passes) were investigated, and they show mostly the same behavior: in the plumes, the whistler mode waves of hiss propagate poleward, away from the magnetic equator, not a single exception was detected. Therefore, the source region of hiss emission is equatorward of the observation location (20–30° magnetic latitude) and most likely in the equatorial region of the plasmaspheric drainage plume, as sketched in Figure 4a.

This present study does not comment on the actual generation mechanism of hiss because Cluster spacecraft do not collect observations in the source region. However, the generation is likely related to the distribution functions of hot electrons which become unstable to whistler mode waves in the equatorial region. It is important to recognize that the particle distribution functions are stable at higher magnetic latitudes because already at 20–30° of magnetic latitude, all waves propagate poleward. It was recently proposed that the dawnside chorus emission generated outside the plasmasphere is the source of plasmaspheric hiss [*Chum and Santolík*, 2005; *Bortnik et al*., 2008; *Meredith et al*., 2013]. However, no chorus emission was observed in these passes, and the present data show that the source of hiss waves lies within the plumes and their interactions with plasma sheet particles.

A puzzling observation is that, in the plasmasphere and plasmapause, the whistler mode waves of hiss emission propagate equatorward even in the case where two spacecraft are at 10° of magnetic latitude in opposite hemispheres. In this case the polar angle of the wave vector can have high values (30–50°), suggesting that these waves are not near their source region but have been refracted. Furthermore, it is unclear what will happen to these waves at the equator. Note that, although the Cluster satellites cross the magnetic equator, the whistler mode waves are hidden by much stronger equatorial noise. Since the whistler mode waves are observed to propagate at large angles on both sides, this strongly suggests that the waves are damped as they approach and cross the magnetic equator. Since the waves are oblique, they have a field-aligned component to the wave electric field, and thus, Landau damping on warm electrons is the most likely mechanism.

Combining the observations in the plumes and plasmasphere region, we suggest that, in the dusk sector, the hiss emission is generated in the equatorial region of the plasmaspheric drainage plumes where the hot particle populations become unstable to whistler mode waves. These waves propagate along the magnetic field lines (in both hemispheres) toward the polar regions, where they are refracted into the plasmasphere and propagate equatorward in both hemispheres. What happens to the whistler mode waves in the plasmasphere when they approach the magnetic equator remains an open question. It is observed that the waves propagate at large angles (up to 50° to the local magnetic field) at 10° magnetic latitude in both hemispheres. These waves must get damped likely via Landau damping on warm electrons around the magnetic equator as they are not observed in the opposite hemisphere.

Acknowledgments
We thank the Cluster Science Archive (http://www.cosmos.esa.int/web/csa) for providing the calibrated Cluster observations.

The Editor thanks James Roeder and Yuri Shprits for their assistance in evaluating this paper.

References

Bortnik, J., R. M. Thorne, and N. P. Meredith (2008), The unexpected origin of plasmaspheric hiss from discrete chorus emissions, *Nature*, *452*(7183), 62–66.

Carpenter, D. L., and R. R. Anderson (1992), An ISEE/whistler model of equatorial electron density in the magnetosphere, *J. Geophys. Res.*, *97*, 1097–1098, doi:10.1029/91JA01548.

Chappell, C. R., K. K. Harris, and G. W. Sharp (1970), A study of the influence of magnetic activity on the location of the plasmapause as measured by OGO 5, *J. Geophys. Res.*, *75*, 50–56, doi:10.1029/JA075i001p00050.

Chum, J., and O. Santolík (2005), Propagation of whistler-mode chorus to low altitudes: Divergent ray trajectories and ground accessibility, *Ann. Geophys.*, *23*, 3727–3738.

Cornilleau-Wehrlin, N., et al. (1997), The Cluster Spatio-Temporal Analysis of Field Fluctuations (STAFF) experiment, *Space Sci. Rev.*, *79*, 107–136.

Darrouzet, F., et al. (2006), Analysis of plasmaspheric plumes: Cluster and IMAGE observations, *Ann. Geophys.*, *24*, 1737–1758.

Darrouzet, F., J. De Keyser, P. M. E. Décréau, F. El Lemdani-Mazouz, and X. Vallieres (2008), Statistical analysis of plasmaspheric plumes with Cluster/WHISPER observations, *Ann. Geophys.*, *26*, 2403–2417, doi:10.5194/angeo-26-2403-2008.

Elphic, R. C., L. A. Weiss, M. F. Thomsen, D. J. McComas, and M. B. Moldwin (1996), Evolution of plasmaspheric ions at geosynchronous orbit during times of high geomagnetic activity, *Geophys. Res. Lett.*, *23*, 2189–2192, doi:10.1029/96GL02085.

Escoubet, C. P., M. Fehringer, and M. Goldstein (2001), Introduction: The Cluster mission, *Ann. Geophys.*, *19*, 1197–1200, doi:10.5194/angeo-19-1197-2001.

Lyons, L. R., and R. M. Thorne (1973), Equilibrium structure of radiation belt electrons, *J. Geophys. Res.*, *78*, 2124–2149.

Meredith, N. P., R. B. Horne, S. A. Glauert, and R. R. Anderson (2007), Slot region electron loss timescales due to plasmaspheric hiss and lightning generated whistlers, *J. Geophys. Res.*, *112*, A08214, doi:10.1029/2006JA012413.

Meredith, N. P., R. B. Horne, J. Bortnik, R. M. Thorne, L. Chen, W. Li, and A. Sicard-Piet (2013), Global statistical evidence for chorus as the embryonic source of plasmaspheric hiss, *Geophys. Res. Lett.*, *40*, 2891–2896, doi:10.1002/grl.50593.

Moldwin, M. B., L. Downward, H. K. Rassoul, R. Amin, and R. R. Anderson (2002), A new model of the location of the plasmapause: CRRES results, *J. Geophys. Res.*, *107*(A11), 1339, doi:10.1029/2001JA009211.

Moldwin, M. B., J. Howard, J. Sanny, J. D. Bocchicchio, H. K. Rassoul, and R. R. Anderson (2004), Plasmaspheric plumes: CRRES observations of enhanced density beyond the plasmapause, *J. Geophys. Res.*, *109*, A05202, doi:10.1029/2003JA010320.

Němec, F., O. Santolík, K. Gereova, E. Macusova, H. Laakso, Y. de Conchy, M. Maksimovic, and N. Cornilleau-Wehrlin (2006), Equatorial noise: Statistical study of its localization and the derived number density, *Adv. Space Res.*, *37*, 610–616.

Santolík, O., and J. Chum (2009), The origin of plasmaspheric hiss, *Science*, *324*(5928), 729–730.

Santolik, O., M. Parrot, and F. Lefeuvre (2003), Singular value decomposition methods for wave propagation analysis, *Radio Sci.*, *38*(1), 1010, doi:10.1029/2000RS002523.

Santolik, O., D. A. Gurnett, J. S. Pickett, S. Grimald, P. M. E. Decreau, M. Parrot, N. Cornilleau-Wehrlin, F. El-Lemdani Mazouz, D. Schriver, and A. Fazakerley (2010), Wave-particle interactions in the equatorial source region of whistler-mode emissions, *J. Geophys. Res.*, *115*, A00F16, doi:10.1029/2009JA015218.

Santolík, O., E. Macúsová, I. Kolmasová, N. Cornilleau-Wehrlin, and Y. de Conchy (2014), Propagation of lower-band whistler-mode waves in the outer Van Allen belt: Systematic analysis of 11 years of multi-component data from the Cluster spacecraft, *Geophys. Res. Lett.*, *41*, 2729–2737, doi:10.1002/2014GL059815.

Summers, D., B. Ni, N. P. Meredith, R. B. Horne, R. M. Thorne, M. B. Moldwin, and R. R. Anderson (2008), Electron scattering by whistler-mode ELF hiss in plasmaspheric plumes, *J. Geophys. Res.*, *113*, A04219, doi:10.1029/2007JA012678.

Thorne, R. M., E. J. Smith, R. K. Burton, and R. E. Holzer (1973), Plasmaspheric hiss, *J. Geophys. Res.*, *78*, 1581–1595, doi:10.1029/JA078i010p01581.

Walsh, B. M., D. G. Sibeck, Y. Nishimura, and V. Angelopoulos (2013), Statistical analysis of the plasmaspheric plume at the magnetopause, *J. Geophys. Res. Lett.*, *118*, 4844–4851, doi:10.1002/jgra.50458.